CV-MMP: max-pressure control for multi-modal traffic in partially connected vehicle environments

Tan, Chaopeng; Rinaldi, Marco; van Lint, Hans

Publication date
2025

Document Version
Accepted author manuscript

Citation (APA)
Tan, C., Rinaldi, M., & van Lint, H. (2025). *CV-MMP: max-pressure control for multi-modal traffic in partially connected vehicle environments*. Paper presented at 104th Annual Meeting of the Transportation Research Board (TRB), Washington DC, District of Columbia, United States.

CV-MMP: Max-pressure control for multi-modal traffic in partially connected vehicle environments

Chaopeng Tan, Ph.D., Postdoc
Department of Transport and Planning
Delft University of Technology
Gebouw 23, Stevinweg 1, 2628 CN, Delft, Netherlands
Email: c.tan-2@tudelft.nl

Marco Rinaldi, Ph.D., Assistant Professor
Corresponding author
Department of Transport and Planning
Delft University of Technology
Gebouw 23, Stevinweg 1, 2628 CN, Delft, Netherlands
Email: m.rinaldi@tudelft.nl

Hans van Lint, Ph.D., Professor
Department of Transport and Planning
Delft University of Technology
Gebouw 23, Stevinweg 1, 2628 CN, Delft, Netherlands
Email: j.w.c.vanlint@tudelft.nl

Word Count: 5913 words + 0 table(s) × 250 = 5913 words

Submission Date: March 12, 2025

ABSTRACT

Among real-time traffic control methods, max-pressure (MP) control stands out due to its simplicity, decentralized nature, and robust theoretical foundation. Besides, advancements in connected vehicle (CV) technology have motivated a significant amount of research into traffic signal control based on CVs. Nevertheless, few studies have been dedicated to MP control in partially CV environments and meanwhile consider multi-modal traffic flows. To fill this research gap, this study proposes CV-based multi-modal MP control (CV-MMP), which calculates the pressure based on travel time information of CVs weighted by vehicle occupancy. Therefore, a hierarchical multi-modal traffic signal priority controller is achieved in a soft manner. Besides, adapting to the requirements of practical applications, CV-MMP is extended to fuse detector data and consider phase switching lost time and cyclic phase sequence. The evaluation results based on a toy network simulation demonstrate that CV-MMP can significantly reduce transit delay with a small increase in private vehicle delay, resulting in a significant reduction in average person delay. In addition, approximately 75% of CBs pass through the network without experiencing delays due to stopping. Therefore, our method can achieve effective transit signal priority and even transit signal coordination under single transit requests.

Keywords: Max-pressure control, Connected vehicle, Multi-modal traffic, Transit signal priority

INTRODUCTION

Traffic signal control is a critical component in managing urban traffic flows, directly impacting travel efficiency, fuel consumption, and urban air pollution (*1–5*). According to the control types, traffic signal control methods can be broadly classified into fixed-time and real-time responsive systems. Fixed-time control is mostly applied to steady traffic flow scenarios, where a fixed signal timing scheme is operated during the time-of-day period (*6*). In contrast, real-time signal control adapts to varying traffic flows by dynamically adjusting signal timing with actuated or adaptive control strategies (*7*).

Among these real-time control methods, the Max-Pressure (MP) control algorithm stands out due to its simplicity, decentralized nature, and robust theoretical foundation (*8*). Unlike centralized systems requiring extensive communication infrastructure, MP control operates effectively with local information, making it scalable and cost-effective. Its decentralized approach allows each intersection to make independent decisions, significantly reducing computational complexity and enhancing resilience to failures. Furthermore, the guarantees of queue stability and throughput optimality for MP control ensure that it can maintain efficient traffic flow even under varying and unpredictable traffic conditions (*9*).

Despite numerous existing studies on MP control, there are still research gaps. On the one hand, the popularity of connected vehicles (CVs) has fostered a large number of studies dedicated to CV-based traffic control (*10–12*), yet only a small number of studies have been dedicated to MP control that is entirely based on CVs and takes full advantage of CV data (*13*). On the other hand, urban road networks need to serve multiple transportation modes, e.g., private cars, buses, and trams, while few studies have considered multi-modal traffic in MP control (*14*). This study will focus on the application of MP control in multi-modal traffic scenarios and is based on CV data only.

Literature review

The original MP calculates "pressure" for each possible signal phase by the difference in the number of vehicles between incoming and outgoing lanes (*8, 9*). The phase with the highest pressure is selected at each time step, effectively pushing traffic through the network in a way that balances demand and reduces overall delay. Subsequent research has focused on improving the original MP in two ways, including pressure calculation and signal implementation. In this section, we will first provide an overview of the various variants of MP control, and then pay special attention to MP control in a partially CV environment and MP control with transit signal priority (TSP).

Variants of MP control

Releasing the ideal assumption of infinite queue capacity by original MP, Gregoire et al., (2015) (*15*) introduced capacity-aware MP control that modifies pressure calculation by incorporating intersection capacity constraints. The use of normalized pressure guarantees work conservation of the control (i.e., at each time step the existence of a non-empty incoming link and a non-full outgoing link is sufficient to ensure that at least one vehicle is served) and mitigates congestion propagation. In order to address the two weaknesses of the original MP, i.e., erratic, unpredictable phase order and requirement of known turning ratios, Le et al., (2015) (*16*) proposed a cyclic MP control with fixed cycle time and unbiased estimates of turning ratios, which still retain the stability property. Considering fairness with respect to delay, Wu et al., (2018) (*17*) proposed a head-of-line vehicle delay-based MP control, which can reduce the excessive delay of vehicles in a small queue

compared to the original MP control. Accounting for the spatial distribution of queues, Li et al., (2019) (*18*) proposed a position-weighted MP that gave higher weights to queues near the ingress of the road, thus reducing the potential of spillback. Considering phase switching loss, Wang et al., (2022) (*19*) extended MP control by introducing a switching rule that reduces the switching frequency according to the congestion level. Particularly, the position-weighted pressure is further optimized by policy-gradient reinforcement learning (RL) algorithms.

These studies have concentrated mainly on analytical models and results of variant MP control, assuming that the traffic flow parameters, e.g., queues and turning ratios, are known, but with little consideration of the difficulties of accurate traffic flow parameter collection in practice. Therefore, Mercader et al., (2020) (*20*) proposed a cyclic travel-time-based MP control with two practical advantages: the travel time is easier to collect than queues and travel-time-based pressure inherently takes into account the capacity of the link.

MP control in CV environments

Recent advances in information technology have made real-time vehicle-to-vehicle (V2V), vehicle-to-infrastructure (V2I), and vehicle-to-cloud (V2C) communications possible. Such vehicles, which can provide real-time location and speed information, are referred to as connected vehicles (CVs). Compared to fixed-location detectors that collect one-dimensional time-series traffic data at specific locations, CVs as mobile detectors can provide two-dimensional spatiotemporal observations of traffic flows, which better reflects the operation of traffic flow. Its mobile detection feature makes the CV data naturally characterized by widespread coverage, making it a cost-effective data source for traffic management. Nevertheless, the most challenging aspect of applying CV data is that it only accounts for a certain penetration rate of the full population of vehicles, i.e., CV data is a sampling observation of the traffic flow. The popularity of CVs in recent years has fostered a large number of studies on traffic state estimation and signal optimization, e.g., network OD/path flow estimation (*21–23*), intersection queue length/delay estimation (*24–28*), and fixed/real-time signal optimization at intersections/arteries/networks (*29–31*).

Regarding MP control, only a few studies have been devoted to CV environments. Based on Little's Law, Dixit et al., (2020) (*32*) related queue length to delay and proposed a crowdsourced delay-based MP control that is suitable for practical implementation. Rather than using point queue models, Liu et al., (2022) (*33*) used a store-and-forward model for traffic evolution and proposed a total delay-based MP control, where the total delay is calculated as the sum of queue length during the period between decision steps. In particular, this method is applicable to partially CV environments, although the stability is proved under 100% CV environment. Utilizing a decentralized RL scheme, Mo et al., (*13*) proposed a CVLight leveraging CV data for adaptive traffic signal control, where the reward is the negative value of the capacity-aware pressure.

MP control for multi-modal traffic

Urban road networks need to serve multiple transportation modes including private cars and public transit. To reduce traffic congestion and lower greenhouse gas emissions, it is necessary to increase ridership by making public transit a more attractive mobility option, by improving the efficiency and reliability of the public transit system. TSP at signalized intersections is one of the common and effective operational strategies. Nevertheless, only a very few studies have considered TSP in the framework of MP control. Xu et al., (2022) (*34*) integrate public TSP into MP control by including hard constraints that give priority for buses. However, the assumption of the existence

of exclusive bus lanes limits the applicable scenarios of the method. Vlachogiannis et al., (2024) (*14*) proposed HumanLight, an RL-based MP control whose reward function employs the concept of pressure at the person level. The method achieves TSP in a soft manner to some extent by rewarding higher occupancy vehicles with travel time savings. However, the method assumes that all vehicles are connected, yet uses queue-based pressure and does not fully exploit the information provided by CV trajectories. In addition, the RL-based scheme limits its portability.

Contributions of this study

To fill the aforementioned research gaps, this study proposes a CV-based MP control for multi-modal traffic at signalized intersections, CV-MMP.

1. The proposed method calculates the pressure by the link travel times of CVs weighted by vehicle occupancy, which is applicable to scenarios with partial CV penetration and enables hierarchical multi-modal traffic signal priority in a soft way.
2. In order to make the proposed CV-MMP control more applicable in practice, we also consider the phase switching lost time and the cyclic phase sequence in a soft way. Besides, we show the potential of CV-MMP to fuse detector data, which make the method adaptable to current road networks with variable detector deployment scenarios.
3. Extensive simulation results show that our method can achieve lower person delay and transit delay, and can even achieve transit signal coordination in the case of a single transit vehicle request. In addition, the method exhibits low sensitivity to errors in occupancy estimation for transit vehicles, demonstrating its robustness against imperfect data.

PRELIMINARIES

Network definition

Without loss of generality, the road traffic network is assumed to have a set $\mathscr{N}$ of signalized intersections indexed by n. As presented in Fig. 1 (a), for each intersection n, $\mathscr{I}_n$ denotes the set of input links indexed by i and $\mathscr{O}_n$ denotes the set of output links indexed by o. (i,o) represents a specific traffic movement, where the first item in this parenthesis indicates the incoming link and the second item indicates the outgoing link. $\cdot_o^i$ denotes the specific traffic parameter related to movement (i,o), e.g., α_o^i denotes the turning ratio of movement (i,o) accounting for the input link i. For brevity, we omit the index used to characterize the time dependence of traffic parameters. When not specified, these parameters refer to the time step t_0 at which the signal timing decision is taken. On the input link of movement (i,o), $\widetilde{\mathscr{V}}_o^i$ denotes the set of CVs with size $\widetilde{x}_o^i$, $\widehat{\mathscr{V}}_o^i$ denotes the set of human-driven vehicles (HV) with size $\widehat{x}_o^i$, and $\mathscr{V}_o^i = \widetilde{\mathscr{V}}_o^i \bigcup \widehat{\mathscr{V}}_o^i$ denotes the set of all vehicles with size $x_o^i = \widetilde{x}_o^i + \widehat{x}_o^i$, both of which are indexed by vehicle v. Regarding each output link o of intersection n, it is also the input link of a neighboring intersection, whose corresponding controlled movements are denoted by set $\mathscr{K}_o$ and indexed by (o,k). Regarding traffic signals, $\mathscr{J}_n$ denotes the set of all signal phases at intersection n, indexed by j. For each phase j, $\mathscr{M}_j$ denotes the set of all permitted movements.

Information provided by CVs

In this study, those vehicles that can provide real-time location and speed information are referred to as CVs. In multi-modal traffic scenarios, CVs are broadly categorized into connected cars (CCs), connected transit vehicles (CTs), and connected emergency vehicles (CEs). Specif-

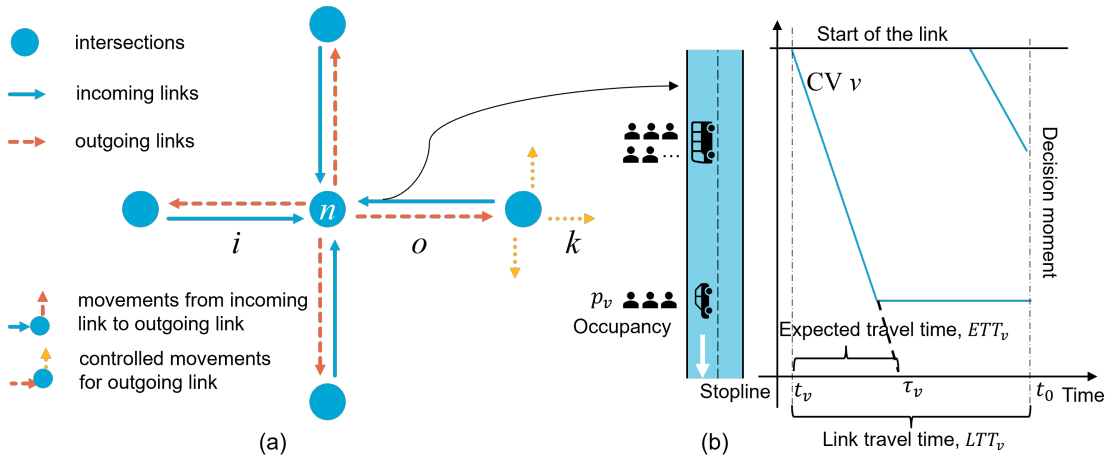

FIGURE 1 (a) Network definition and (b) information provided by CVs.

ically, CCs comprise those private or commercial (e.g., shared mobility vehicles) vehicles using navigation services, which share their positioning information with map companies for travel route planning. In particular, CCs only account for a certain ratio of all vehicles. CTs include all types of public transport modes on urban roads, e.g., buses and trams, all of which are already connected to implement transit priority or time-of-arrival optimization. CEs refer to ambulances and fire trucks, which are also connected for real-time dispatching needs. In addition to trajectory information, throughout this study we also assume that CVs can provide occupancy information, i.e., the number of passengers (including the driver) in the vehicle. For CCs, such information can be shared by drivers when using navigation services, while for CTs, the occupancy can be estimated by the boarding and alighting data (*35, 36*).

Fig. 1 (b) illustrates the real-time trajectories of CVs on the link. For each CV $v \in \tilde{\mathscr{V}}_o^i$, we can easily extract its real-time link travel time LTT_v,

$$LTT_v = t_0 - t_v, \tag{1}$$

where t_0 is the time step t_0 at which the signal timing decision is taken and t_v is the moment when the CV entered the link. The expected travel time ETT_v is calculated as

$$ETT_v = \tau_v - t_v, \tag{2}$$

where τ_v is the projected arrival time of CV v, which can be easily estimated by the CV trajectory (*37*). Meanwhile, each CV can provide its occupancy information p_v (person). Then, the total person travel time PTT_v of each CV is calculated as

$$PTT_v = p_v \cdot LTT_v. \tag{3}$$

METHODOLOGY

In this section, we first summarize two types of MP control with different phase switching modes, non-cyclic MP and cyclic MP. The former activates the phase with the highest pressure at each decision step, resulting in a randomized phase order. The latter, on the other hand, switches phases under the constraint of a pre-defined phase sequence. Then, we propose a CV-based MP control method, CV-MMP, that is non-cyclic yet considers phase sequences as much as possible, utilizes

CV information for pressure calculation, and considers multi-modal traffic flows at intersections in a soft manner.

Non-cyclic MP

A non-cyclic MP control activates the phase with the maximum pressure at each decision time step, where the phase pressure is calculated as the sum of the product of the weight and saturation flow rate for each served movement. The original MP control calculates the movement weight as the difference between the upstream link queue (point queue, i.e., the number of vehicles) and the average downstream link queue weighted by the turning ratios (*9*). Later research on variants of MP control has focused on exploring the traffic state metrics chosen for pressure calculations, e.g., position-weighted queue (*18*), travel time (*20*), head-of-line delay (*17*), or vehicle delay (*33*).

In general, a non-cyclic MP control can be expressed as follows:

$$j^* = \arg\max_{j \in \mathscr{J}_n} P_j, \tag{4}$$

$$\text{where} \quad P_j = \sum_{(i,o) \in \mathscr{M}_j} w_o^i c_o^i \tag{5}$$

$$\text{and} \quad w_o^i = b_o^i - \sum_{(o,k) \in \mathscr{K}_o} \alpha_k^o b_k^o. \tag{6}$$

Eq. (4) activates the phase j^* with maximum pressure P_j; Eq. (5) calculates the pressure of each phase j, where w_o^i denotes the movement weights and c_o^i denotes the saturated departure rate. Eq. (6) calculates the movement weights. b_o^i is the selected traffic state metric (e.g. pressure, or delay) of movement (i,o) (i.e., the upstream link) and $\sum_{(o,k) \in \mathscr{K}_o} \alpha_k^o b_k^o$ is the corresponding average value of the downstream link weighted by turning ratios α_k^o.

Cyclic MP

Non-cyclic MP control, although it can achieve better performance by switching phases flexibly, may be contrary to the driver's expectation, which means that the driver anticipates the switching of phases through experience and prepares the vehicle to start in advance. Moreover, a cyclic signal timing is also more friendly to pedestrians crossing the street, especially at intersections with unbalanced traffic. Therefore, some studies propose cyclic MP control with a pre-defined phase sequence.

Typically, the calculation of weights and pressures for cyclic MP control is similar to that for non-cyclic MP control, with the main difference being the way in which the green phase is determined. Currently, there are two main types of approaches to determining the green time for cyclic MP control: one is optimization-based methods that maximize pressure over a long future period, where hard constraints on the given phase sequence are included (*38*). The other allocates the effective green time based on the proportion of pressure to the overall total as follows (*16*):

$$g_j^* = \varphi_j G_n \quad \text{where} \quad \varphi_j = \frac{f(P_j)}{\sum_{j \in \mathscr{J}_n} f(P_j)}, \tag{7}$$

where g_j^* is the allocated green time to phase j. G_n is the total effective green time (Mercader et al. (*20*) exclude minimum green time in G_n, thus g_j^* needs to add minimum green time in such a case). φ_j is the proportion determined by phase pressure. $f(P_j)$ denotes the function of P_j, e.g., $f(P_j) = P_j$ (*20*) or $f(P_j) = e^{\eta P_j}$ with parameter η controlling the differences in green ratios (*16*).

CV-MMP: CV-based multi-modal MP control

CV travel time-based weights

In our partially CV environment, we use the normalized total person travel time to calculate the movement weight in Eq. (6), then we have

$$w_o^i = \frac{\sum_{v \in \tilde{\mathscr{V}}_o^i} PTT_v}{\overline{ETT}^i} - \frac{\sum_{(o,k) \in \mathscr{K}_o} \alpha_k^o \sum_{v' \in \tilde{\mathscr{V}}_k^o} PTT_{v'}}{\overline{ETT}^o}. \tag{8}$$

where $\sum_{v \in \tilde{\mathscr{V}}_o^i} PTT_v$ calculates the total travel time of CVs of movement (i,o), which is weighted by occupancy information. $\overline{ETT}^i$ is the expected travel time of link i, which can be estimated as the average ETT_v of historical CVs on this link during the same time-of-day period. Considering instead turning ratios α_k^o, these could also be calibrated by the historical average turning ratio of CVs, assuming adequate penetration rates (*39*).

Here we clarify *three significant advantages* of using normalized vehicle travel time information for weight calculation. First, similar to the TD-MP (*40*) which calculated weights by vehicle delay, the vehicle travel time information also reflects the cumulative delay incurred by vehicles, which prevents vehicles in movements with low demand from experiencing excessive delays and improves delay equity. Second, compared to delay-based pressure weights considering stopped vehicles only, travel time-based pressure weights also consider moving vehicles, which more comprehensively characterizes the link traffic state. Third, by normalizing the link total travel time with expected travel time, our weights take into account the capacity of the link to some extent since the link travel time and link length are positively correlated.

Phase pressure considering lost time

For non-cyclic MP control, we can only determine the next phase at each decision step. Therefore, when the next phase is different from the current phase, a phase transition period consisting of yellow and red clearance time needs to be inserted for safety reasons in practical application, which brings lost time to the next phase, as presented in Fig. 2.

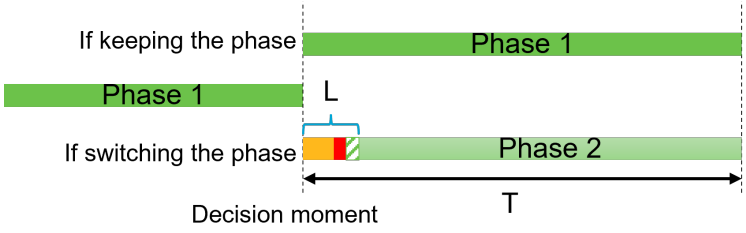

FIGURE 2 Phase switching lost time.

Referring to Levin et al. (*38*) and Liu and Gayah (*40*), with consideration of phase switching lost time, a lost time parameter δ_o^i is added in Eq. (5) to discount c_o^i as follows:

$$P_j = \sum_{(i,o) \in \mathscr{M}_j} w_o^i \delta_o^i c_o^i \quad \text{and} \quad \delta_o^i = \begin{cases} 1 & \text{if} \quad (i,o) \in \mathscr{M}_{j_{last}^*} \\ 1 - L/T & \text{if} \quad (i,o) \notin \mathscr{M}_{j_{last}^*} \end{cases} \tag{9}$$

where T is the length of decision steps. L is the phase switching lost time including yellow time, red clearance time if applicable, and green start lost time. j_{last}^* represents the activated phase

at the last decision step. When $(i,o) \in \mathscr{M}_{j^*_{last}}$, i.e., the next activated phase is the same as the current phase, it is essentially an extension of the green time of the current phase, leading to no lost time. Otherwise, the effective green time of the next activated phase becomes $T-L$, leading to a discounted saturated departure rate, i.e., $(1-L/T)c^i_o$. Especially, the consideration of phase transition lost time poses a constraint on T, i.e., $T > L$.

Activating phase with consideration of phase sequence

Note that existing cyclic MP control activates phases with hard constraints on a pre-defined phase sequence, which may result in sub-optimal allocation of green time to low-demand movements. However, we would also like the phase sequence to not be completely chaotic as in the case of non-cyclic MP control, in order to be more pedestrian-friendly and not betray the expectations of of the drivers excessively. Therefore, this study proposes a soft sequential activation approach in the framework of non-cyclic MP control to activate the phases in the specified phase sequence as much as possible. Note that P_j may be negative when the downstream link is more congested than the upstream link. Here we standardize them to positive values as follows

$$P'_j = P_j - \min\{P_{j'} | j' \in \mathscr{J}_n\} + 1 \tag{10}$$

Note that, this standardization process does not change the relative magnitudes of the pressures as well as the differences between them. Then, given standardized phase pressures P'_j and phase sequence $\mathscr{J}_n = \{j^*_{last}, j_1, j_2, \cdots, j_Z\}$ at intersection n, we activate phase j^* based on the following activation approach,

$$j^* = \arg\max_{j \in \mathscr{J}_n} \{P'_{j^*_{last}}, P'_{j_1}, \beta P'_{j_2}, \cdots, \beta^{Z-1} P'_{j_Z}\} \tag{11}$$

where β is an activation parameter determining the flexibility of the phase sequence and $\beta \in [0,1]$. A greater β will result in a more flexible phase sequence. Obviously, if $\beta = 1$, then the approach becomes a non-cyclic MP control as each phase has an equal chance of being activated. If $\beta = 0$, then the phase will be activated strictly in the given phase sequence without any phase skipping. Actually, β^{Z-1} can also be understood as a preference parameter of phase j_Z related to the phase sequence.

The advantage of the soft activation approach proposed in this study is that it preserves the flexibility of phases in a few extreme scenarios (e.g., very uneven traffic) while enabling phases to be executed in the expected sequences in most regular scenarios. By adjusting the activation parameter β, traffic engineers can easily decide the degree of phase flexibility, achieving a tradeoff between control benefits and phase flexibility.

Fusing fixed-location detector data

The store-and-forward queuing model can be used to derive the dynamic queue length on each link o of the network (i.e., the number of vehicles) based on flow conservation (*9, 16, 38*).

$$\begin{aligned} x^o_k(t+1) = x^o_k(t) + d^o_k(t) + \sum_{i \in \mathscr{I}_n} \alpha^o_k(t)[x^i_o(t) \wedge \gamma^i_o(t)\delta^i_o(t)c^i_o(t)] \\ - [x^o_k(t) \wedge \gamma^o_k(t)\delta^o_k(t)c^o_k(t)], \end{aligned} \tag{12}$$

where $x \wedge y = min\{x,y\}$. $x^o_k(t)$ denotes the number of vehicles of movement (o,k) at time step t (for brevity we omit time step hereafter). d^o_k denotes the exogenous demand of movement (o,k) from input links. Binary variable γ^o_k denotes the signal state of movement (o,k). $\gamma^o_k = 1$ if its green

phase is activated and otherwise 0. The third term on the right hand side indicates the vehicles from the upstream intersection and the fourth term indicates the vehicles getting through the current intersection. This queuing model implicitly assumes that the exogenous demand $d_k^o(t)$, turning ratios $\alpha_k^o(t)$, and saturated departure rate $c_k^o(t)$ are known, whereas both need to be measured or estimated in practical applications.

Here we assume that fixed-location detectors are deployed near the stopline of signalized intersections, based on which $d_k^o(t)$, $\alpha_k^o(t)$, and $c_k^o(t)$ are measured in real-time. Note that, although some detectors on some links may malfunction, we can still estimate their outputs from the CV data, considering the broad coverage of CVs. There have been a large number of studies focusing on the problem of estimating the traffic state of a road network based on CVs or fused CVs and detectors, including traffic volume/density, queue length, etc (*24–26*). Considering that traffic state estimation is not the focus of this study, we assume that the number of vehicles on the link, i.e., $x_k^o(t)$, is obtained in real-time by fusing CV and fixed-location detectors.

Given the total number of vehicles x_o^i and the number of CVs $\widetilde{x}_o^i$ of movement (i,o), the number of HV is calculated as $\widehat{x}_o^i = x_o^i - \widetilde{x}_o^i$. Then, we extend the Eq. (8) into a more general form integrating both CV and HV information:

$$w_o^i = \frac{\sum_{v\in\widetilde{\mathscr{V}}_o^i} PTT_v + \widehat{x}_o^i \overline{ETT}^i}{\overline{ETT}^i} - \frac{\sum_{(o,k)\in\mathscr{K}_o} \alpha_k^o \left[\sum_{v'\in\widetilde{\mathscr{V}}_k^o} PTT_{v'} + \widehat{x}_k^o \overline{ETT}^o\right]}{\overline{ETT}^o}. \tag{13}$$

where the term $\sum_{v\in\widetilde{\mathscr{V}}_o^i} PTT_v + \widehat{x}_o^i \overline{ETT}^i$ calculates the total travel time of all vehicles of movement (i,o). Note that, since we have no detailed trajectory and occupancy information of HVs, we assume that the travel time of each HV is the expected travel time $\overline{ETT}^i$ of the link and the occupancy is 1. The calculation of the pressure, Eq. (9), and the phase activation function, Eq. (11), for the proposed CV-MMP with detector data remain unchanged.

We consider two extreme cases: (i) if all vehicles are CVs, Eq. (13) is the same as Eq. (8) as $\widehat{x}_o^i = 0$, then the method becomes a complete person travel time-based MP control. (ii) If all vehicles are HVs, Eq. (13) becomes

$$w_o^i = x_o^i - \sum_{(o,k)\in\mathscr{K}_o} \alpha_k^o x_k^o$$

as $\widetilde{\mathscr{V}}_o^i$ is empty, then the method degenerates into the original MP control. This implies that our method may have inherited the two properties of stability and maximum throughput of the original MP control, although further theoretical proof is needed in future study.

EVALUATION

In this section, we test the CV-MMP with fusing detector data, with accurate occupancy information, with considering lost time, and without considering phase sequence as default. The following variants of CV-MMP are compared to isolate the effects of each component: (i) without occupancy information, i.e., letting p_v of all CVs be 1 in Eq. (3), (ii) with inaccurate occupancy information, i.e., adding random errors to p_v of CBs, (iii) without considering lost time, i.e., letting $\delta_o^i = 1$ for all movements in Eq. (9), (iv) without fusing detector data, i.e., calculating weights by Eq. (8), (v) with considering phase sequence, i.e., activating the phase by Eq. (11).

Toy network

The proposed CV-MMP control method is evaluated in a toy network with five intersections in DLR SUMO (*41*), including one center intersection and four perimeter intersections, as illustrated in Fig. 3. Each intersection consists of four links and each link comprises three lanes for different turning directions, i.e., left turn, straight through, and right turn. The turn ratios for the straight-through and left-turn directions are centered at 0.55 and 0.25 respectively, accompanied by deviations following a normal distribution. Vehicle inputs at peripheral links follow Poisson distributions with arrival rates ranging from 0.13-0.18 veh/s. In total, the input volume of the whole network is about 6700 veh/h, corresponding to a demand-to-capacity ratio (d/c) of about 0.8.

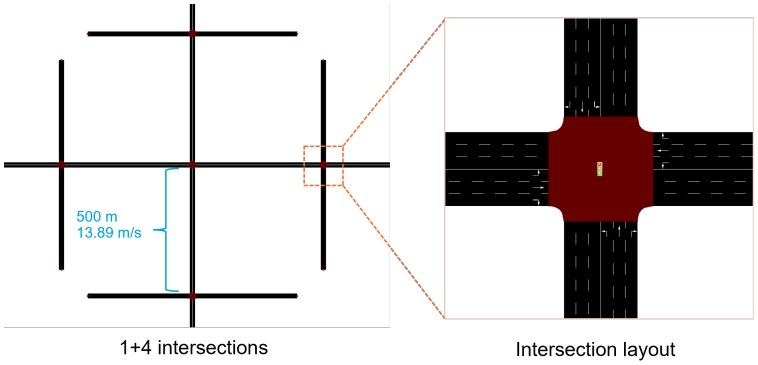

FIGURE 3 Toy network simulation.

Two types of connected vehicles are included in the 60 min simulation, connected buses (CBs) and connected cars (CCs). The occupancy (including the driver) of CBs ranges from 16–86, while that of CCs ranges from 2–5. Regarding HVs, since they are not connected, occupancy defaults to 1. Under different test scenarios, the penetration rate of CBs is fixed at 3% and the penetration rate of CCs varies from 0.1–0.9. Considering the phase switching lost time, including 3 seconds of yellow time and 2 seconds of green start lost time, the decision step for CV-MMP is set to be 10 s.

Result analysis

With and without occupancy information

This section compares the performance of CV-MMP control with and without occupancy information. Note that delay here refers to the control delay, i.e., the total time loss of a vehicle due to the signal control. From Fig. 4 (a) and (b), we can find that:

a. With increasing CC penetration rates, both average vehicle and person delay decrease for CV-MMP without occupancy information. Besides, the vehicle delay is almost the same as the person delay under various penetration rates.
b. With increasing CC penetration rates, the average vehicle delay decreases while the average person delay increases for CV-MMP with occupancy information. Besides, the average person delay is significantly less than the average vehicle delay, though such differences decrease with increasing CC penetration rates.
c. Compared to CV-MMP without occupancy information, though the average vehicle delay of CV-MMP with occupancy information increases by 4–6 s/vehicle, the average

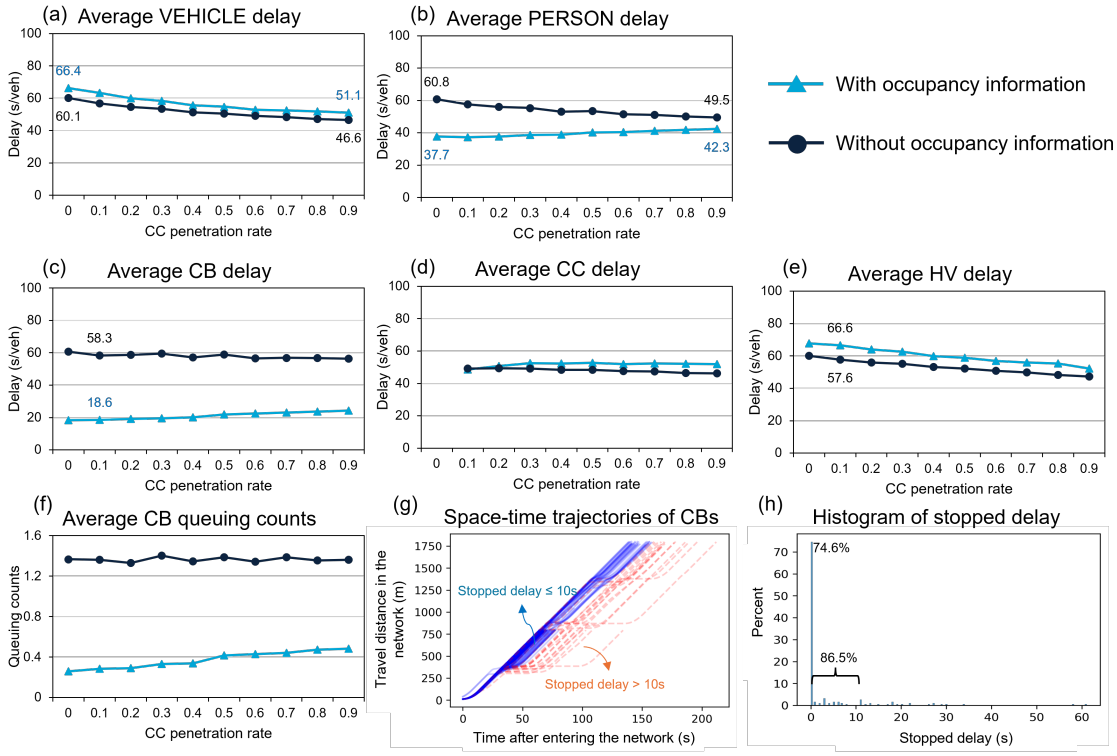

FIGURE 4 CV-MMP performance with and without occupancy information.

person delay decreases significantly, varying from 7–23 s/person as CC penetration rate decreases.

The above results can be interpreted by the detailed performance of each type of vehicle presented in Fig. 4 (c)–(e):

d. After utilizing occupancy information, the proposed CV-MMP control significantly reduces the delay of those CVs with high occupancy, i.e., CBs, accompanied by a very small sacrifice of delay of the other vehicles, i.e., CCs and HVs. For instance, at a 0.1 penetration rate of CCs, the average CB delay decreases by almost 68.1%, while the average HV delay only increases by 15.6% and the average CC delay almost has no change.

In terms of the number of vehicles, CBs only accounted for 3% of the total, and after CV-MMP utilizing the occupancy information, the average vehicle delay still increased due to the increase in other vehicle (accounting for 97%) delays, even though CB delays were significantly reduced. As for the person delay, since the occupancy of CB is very high, the total person delay of CBs is also high as a percentage of the total, so the decrease in CB delay can lead to a significant decrease in average person delay.

In Fig. 4 (f)–(h), we further provide some detailed results on the performance of CBs. Fig. 4 (f) shows that, similar to the average CB delay presented in Fig. 4 (c), average CB queuing counts are also significantly reduced under various CC penetration rates considering CV-MMP utilizing occupancy information. Fig. 4 (g) presents the detailed space-time trajectories of CBs at a 0.3 CC penetration rate, where solid lines represent CBs with stopped delay (the duration when the vehicle speed is 0) no more than 10 s and dashed lines represent CBs with stopped delay greater than 10 s. Fig. 4 (h) presents the percentage of CBs for different stopped delays. As shown, 74.6% of CBs

did not experience a stopped delay and 86.5% of CBs experienced a stopped delay of no more than 10 s. These results suggest that:

e. The proposed CV-MMP control with occupancy information can significantly reduce the average delay and queuing counts of CBs and thus achieves TSP in a soft manner. When there are no conflicting transit requests, the proposed CV-MMP control can even achieve CB signal coordination on arbitrary paths, i.e., CBs experiencing no stopped delays without pre-defining coordinated paths.

Impact of CB occupancy errors

In practical application, the occupancy information of transit vehicles normally needs to be estimated, which suffers from inevitable errors (*35*). Therefore, in this section, we test the performance of the proposed CV-MMP control with inaccurate occupancy information, where the CC penetration rate is 0.2. Here we added random errors on bus occupancy to model estimation errors, which follow Normal distributions $Normal(0, \sigma^2)$. Fig. 5 presents the average delay of CBs, vehicles, and persons under varying σ. Note that $\sigma = 0$ represents the case with accurate occupancy information. We can find:

f. The proposed CV-MMP control is robust to occupancy errors of transit vehicles as both average CB, vehicle, and person delay almost remain unchanged across varying σ.

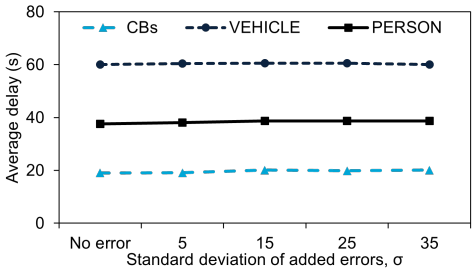

FIGURE 5 Impact of occupancy errors.

With and without considering lost time

Note that disregarding the lost time does not mean that we ignore the phase transition period (yellow time and red clearing time), but rather that we do not take into account the discounting of the saturated departure rate due to the phase switching lost time, i.e., $\delta_o^i = 1$ for all movements when calculating the phase pressure based on Eq. (9). Fig. 6 presents the results of CV-MMP with and without considering phase switching lost time and we find that:

g. Compared to CV-MMP without considering lost time, considering lost time can improve both average vehicle and person delay under various CC penetration rates. This is because, as evidenced by Fig. 6 (c), considering lost time can significantly reduce the number of phase switching under various CC penetration rates, thus raising the cumulative effective green time of the whole road network.

With and without fusing detector data

This section evaluates the performance of CV-MMP in scenarios with and without fusing detector data. As shown in Fig. 7 (a) and (b):

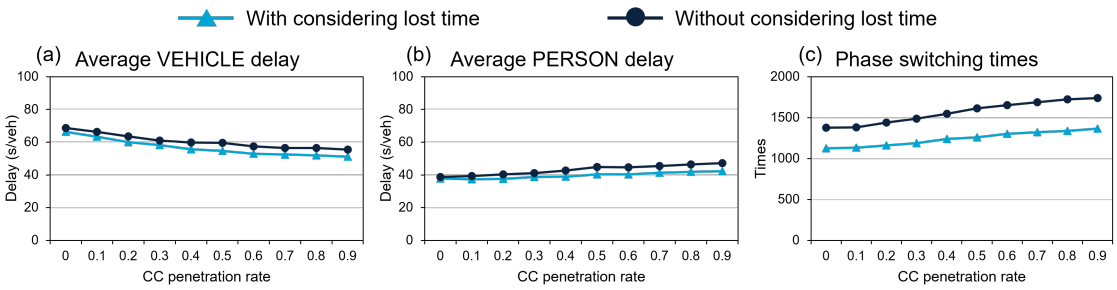

FIGURE 6 CV-MMP performance with and without considering lost time.

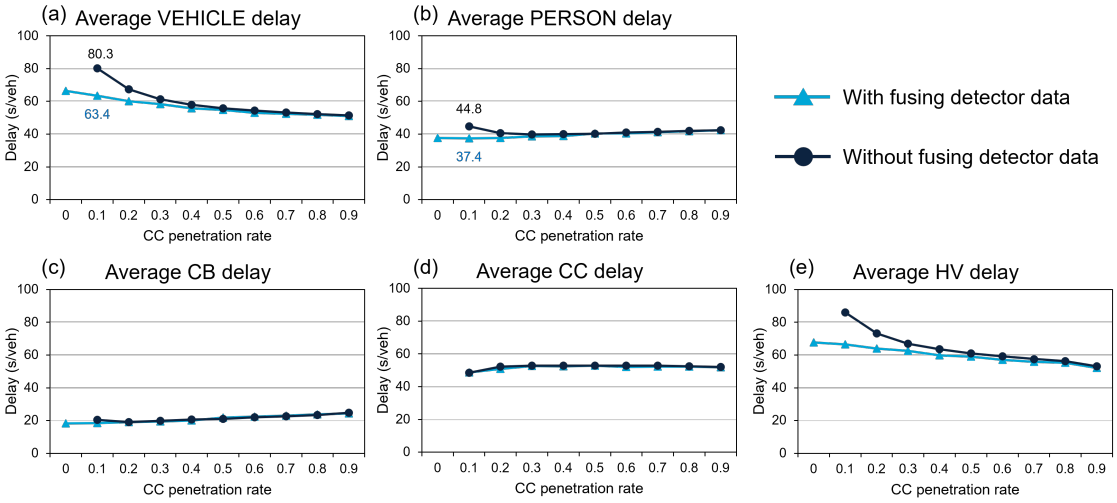

FIGURE 7 CV-MMP performance with and without fusing detector data.

h. By fusing detector data, both the average vehicle and person delays of CV-MMP are improved under various CC penetration rates. Such improvements are more significant under lower CC penetration rates. When the CC penetration rate is 0.1, the improvements of the average vehicle and person delays reach 21% and 16.5%, respectively.

Fig. 7 (c)–(e) shows that:

i. The average CB and CC delays are almost the same under various CC penetration rates for CV-MMP with and without fusing detector data, while the average HV delay significantly decreases after CV-MMP fusing detector data. This suggests that fusing the detector data mainly improves the efficiency of the HV and has less effect on the CV.

j. When the CC penetration rate reaches 30%, the CV-MMP control can then discard the detector data for traffic signal control altogether, as the fusing detector data produces very limited marginal benefit beyond this point.

With and without considering phase sequence

This section evaluates the effect of the proposed soft sequential activation approach, where different values of activation parameter β are tested at a CC penetration rate of 0.3. Recall that, $\beta = 1$ and $\beta = 0$ represent two extreme cases: completely non-cyclic and completely cyclic. The ratio of disordered switching is used to indicate the ratio of incorrect switching that violates the prede-

fined phase sequence, which can equally be interpreted as the proportion of the decisions skipping phases. As shown in Fig. 8:

k. With the activation parameter decreasing from 1 to 0, the ratio of disordered switching almost decreases linearly from 0.56 to 0, while the average delay of CBs increases gradually from 19.5 s/CB to 42.5 s/CB. Since the traffic is more balanced across links in our scenario, the performance of CBs is mainly affected when considering a cyclic phase sequence, under which, some CBs are forced to wait for one more phase, thus increasing the number of CB queuing counts and delays.

l. We suggest adopting a β between 0.5–0.6 for a tradeoff between the CB performance and the ratio of disordered switching. At these points, the ratio of disordered switching decreases to within 25%, and the average CB delay increases by only 18%.

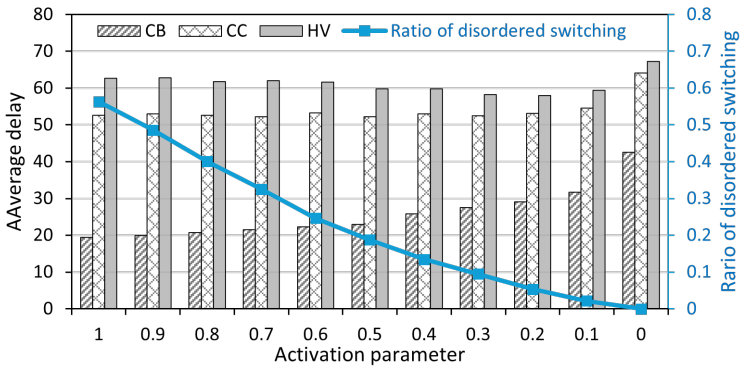

FIGURE 8 CV-MMP performance with and without considering phase sequence.

CONCLUSION AND FUTURE WORK

To fill the research gap that few studies have considered multi-modal traffic for MP control in partially CV environments, this study proposed CV-MMP control, which calculated the pressure based on the travel time of CVs weighted by their occupancy information. In particular, considering the requirements of practical applications, we further consider the phase switching lost time and cyclic phase sequence by introducing a lost time parameter and an activation parameter. Besides, CV-MMP has the potential to fuse fixed-location detector data for enhanced performance under low-penetration-rate CV environments, adapting to variable detector deployment scenarios in current road networks.

Extensive simulation tests on a toy network demonstrated that (i) CV-MMP significantly reduces average delay (e.g., -68.1% at 0.1 CC penetration rate) for high-occupancy vehicles, such as buses, with limited increase (+15.6%) in low-occupancy vehicles, i.e., private cars, leading to a significant reduction in average person delay (-35.2%). (ii) CV-MMP can even enable transit signal coordination, as the majority (about 75%) of buses do not experience stopped delays in the network. This can also be demonstrated by the significant reduction in the number of queuing counts of buses (-79% at 0.1 CC penetration rate). (iii) After considering the phase switching lost time, the performance of CV-MMP can be further improved due to the reduced phase switching frequency. (iv) Fusing fixed-location detector data can also enhance the performance of CV-MMP, mainly in scenarios with CC penetration rates less than 0.3. (v) By introducing an activation

parameter, the CV-MMP can combine both cyclic and non-cyclic phase switching, achieving a tradeoff between the bus performance and the ratio of disordered switching.

There are several possible future research directions. First, theoretical proofs of the stability and maximum throughput of the proposed CV-MMP control are required. Second, we need to test the performance of CV-MMP based on a real road network under various traffic scenarios (e.g., containing a wider variety of vehicles including cars, buses, trams, and emergency vehicles) and unbalanced traffic flows.

AUTHOR CONTRIBUTIONS

The authors confirm their contribution to the paper as follows: study conception: Marco Rinaldi; methodology design: Chaopeng Tan; data collection: Chaopeng Tan; analysis and interpretation of results: Chaopeng Tan, Marco Rinaldi; draft manuscript preparation: Chaopeng Tan, Marco Rinaldi, Hans van Lint; funding acquisition: Hans van Lint, Marco Rinaldi. All authors reviewed the results and approved the final version of the manuscript.

ACKNOWLEDGEMENT

The authors would like to acknowledge the financial contribution of the EU Horizon Europe Research and Innovation Programme, Grant Agreement No. 101103808 ACUMEN.

REFERENCES

1. Guo, Q., L. Li, and X. J. Ban, Urban traffic signal control with connected and automated vehicles: A survey. *Transportation research part C: emerging technologies*, Vol. 101, 2019, pp. 313–334.
2. Kwak, J., B. Park, and J. Lee, Evaluating the impacts of urban corridor traffic signal optimization on vehicle emissions and fuel consumption. *Transportation Planning and Technology*, Vol. 35, No. 2, 2012, pp. 145–160.
3. Boukerche, A., D. Zhong, and P. Sun, Feco: An efficient deep reinforcement learning-based fuel-economic traffic signal control scheme. *IEEE Transactions on Sustainable Computing*, Vol. 7, No. 1, 2021, pp. 144–156.
4. De Coensel, B., A. Can, B. Degraeuwe, I. De Vlieger, and D. Botteldooren, Effects of traffic signal coordination on noise and air pollutant emissions. *Environmental Modelling & Software*, Vol. 35, 2012, pp. 74–83.
5. Coelho, M. C., T. L. Farias, and N. M. Rouphail, Impact of speed control traffic signals on pollutant emissions. *Transportation Research Part D: Transport and Environment*, Vol. 10, No. 4, 2005, pp. 323–340.
6. Tan, C., Y. Cao, X. Ban, and K. Tang, Connected Vehicle Data-Driven Fixed-Time Traffic Signal Control Considering Cyclic Time-Dependent Vehicle Arrivals Based on Cumulative Flow Diagram. *IEEE Transactions on Intelligent Transportation Systems*, 2024.
7. Qadri, S. S. S. M., M. A. Gökçe, and E. Öner, State-of-art review of traffic signal control methods: challenges and opportunities. *European transport research review*, Vol. 12, 2020, pp. 1–23.
8. Varaiya, P., The max-pressure controller for arbitrary networks of signalized intersections. In *Advances in dynamic network modeling in complex transportation systems*, Springer, 2013, pp. 27–66.

9. Varaiya, P., Max pressure control of a network of signalized intersections. *Transportation Research Part C: Emerging Technologies*, Vol. 36, 2013, pp. 177–195.
10. Feng, Y., K. L. Head, S. Khoshmagham, and M. Zamanipour, A real-time adaptive signal control in a connected vehicle environment. *Transportation Research Part C: Emerging Technologies*, Vol. 55, 2015, pp. 460–473.
11. Li, W. and X. Ban, Connected vehicles based traffic signal timing optimization. *IEEE Transactions on Intelligent Transportation Systems*, Vol. 20, No. 12, 2018, pp. 4354–4366.
12. Tan, C. and K. Yang, Privacy-preserving adaptive traffic signal control in a connected vehicle environment. *Transportation research part C: emerging technologies*, Vol. 158, 2024, p. 104453.
13. Mo, Z., W. Li, Y. Fu, K. Ruan, and X. Di, CVLight: Decentralized learning for adaptive traffic signal control with connected vehicles. *Transportation research part C: emerging technologies*, Vol. 141, 2022, p. 103728.
14. Vlachogiannis, D. M., H. Wei, S. Moura, and J. Macfarlane, HumanLight: Incentivizing ridesharing via human-centric deep reinforcement learning in traffic signal control. *Transportation Research Part C: Emerging Technologies*, Vol. 162, 2024, p. 104593.
15. Gregoire, J., X. Qian, E. Frazzoli, A. De La Fortelle, and T. Wongpiromsarn, Capacity-aware backpressure traffic signal control. *IEEE Transactions on Control of Network Systems*, Vol. 2, No. 2, 2014, pp. 164–173.
16. Le, T., P. Kovács, N. Walton, H. L. Vu, L. L. Andrew, and S. S. Hoogendoorn, Decentralized signal control for urban road networks. *Transportation Research Part C: Emerging Technologies*, Vol. 58, 2015, pp. 431–450.
17. Wu, J., D. Ghosal, M. Zhang, and C.-N. Chuah, Delay-based traffic signal control for throughput optimality and fairness at an isolated intersection. *IEEE Transactions on Vehicular Technology*, Vol. 67, No. 2, 2018, pp. 896–909.
18. Li, L. and S. E. Jabari, Position weighted backpressure intersection control for urban networks. *Transportation Research Part B: Methodological*, Vol. 128, 2019, pp. 435–461.
19. Wang, X., Y. Yin, Y. Feng, and H. X. Liu, Learning the max pressure control for urban traffic networks considering the phase switching loss. *Transportation Research Part C: Emerging Technologies*, Vol. 140, 2022, p. 103670.
20. Mercader, P., W. Uwayid, and J. Haddad, Max-pressure traffic controller based on travel times: An experimental analysis. *Transportation Research Part C: Emerging Technologies*, Vol. 110, 2020, pp. 275–290.
21. Cao, Y., K. Tang, J. Sun, and Y. Ji, Day-to-day dynamic origin–destination flow estimation using connected vehicle trajectories and automatic vehicle identification data. *Transportation Research Part C: Emerging Technologies*, Vol. 129, 2021, p. 103241.
22. Wang, Q., Y. Yuan, Q. Zhang, and X. T. Yang, Signalized arterial origin-destination flow estimation using flawed vehicle trajectories: A self-supervised learning approach without ground truth. *Transportation Research Part C: Emerging Technologies*, Vol. 145, 2022, p. 103917.
23. Ma, W., J. Yuan, K. An, and C. Yu, Route flow estimation based on the fusion of probe vehicle trajectory and automated vehicle identification data. *Transportation Research Part C: Emerging Technologies*, Vol. 144, 2022, p. 103907.

24. Zheng, J. and H. X. Liu, Estimating traffic volumes for signalized intersections using connected vehicle data. *Transportation Research Part C: Emerging Technologies*, Vol. 79, 2017, pp. 347–362.
25. Comert, G. and M. Cetin, Analytical evaluation of the error in queue length estimation at traffic signals from probe vehicle data. *IEEE Transactions on Intelligent Transportation Systems*, Vol. 12, No. 2, 2011, pp. 563–573.
26. Tan, C., J. Yao, K. Tang, and J. Sun, Cycle-based queue length estimation for signalized intersections using sparse vehicle trajectory data. *IEEE Transactions on Intelligent Transportation Systems*, Vol. 22, No. 1, 2019, pp. 91–106.
27. Tan, C., J. Yao, X. Ban, and K. Tang, Cumulative flow diagram estimation and prediction based on sampled vehicle trajectories at signalized intersections. *IEEE Transactions on Intelligent Transportation Systems*, Vol. 23, No. 8, 2021, pp. 11325–11337.
28. Tan, C., J. Yao, K. Tang, et al., Joint estimation of multi-phase traffic demands at signalized intersections based on connected vehicle trajectories. *arXiv preprint arXiv:2210.10516*, 2022.
29. Tan, C., Y. Ding, K. Yang, H. Zhu, and K. Tang, Connected Vehicle Data-driven Robust Optimization for Traffic Signal Timing: Modeling Traffic Flow Variability and Errors. *arXiv preprint arXiv:2406.14108*, 2024.
30. Yao, J., C. Tan, and K. Tang, An optimization model for arterial coordination control based on sampled vehicle trajectories: The STREAM model. *Transportation research part C: emerging technologies*, Vol. 109, 2019, pp. 211–232.
31. Al Islam, S. B., A. Hajbabaie, and H. A. Aziz, A real-time network-level traffic signal control methodology with partial connected vehicle information. *Transportation Research Part C: Emerging Technologies*, Vol. 121, 2020, p. 102830.
32. Dixit, V., D. J. Nair, S. Chand, and M. W. Levin, A simple crowdsourced delay-based traffic signal control. *PLoS one*, Vol. 15, No. 4, 2020, p. e0230598.
33. Liu, H. and V. V. Gayah, A novel max pressure algorithm based on traffic delay. *Transportation Research Part C: Emerging Technologies*, Vol. 143, 2022, p. 103803.
34. Xu, T., S. Barman, M. W. Levin, R. Chen, and T. Li, Integrating public transit signal priority into max-pressure signal control: Methodology and simulation study on a downtown network. *Transportation Research Part C: Emerging Technologies*, Vol. 138, 2022, p. 103614.
35. Özgün, K., M. Günay, D. Başaran, and J. Ledet, Estimation of alighting counts for public transportation vehicle occupancy levels using reverse direction boarding. *Journal of Public Transportation*, Vol. 25, 2023, p. 100070.
36. Zhu, M., W. Zhu, J. M. Lutin, Z. Cui, and Y. Wang, Developing a practical method to compute state-level bus occupancy rate. *Journal of Transportation Engineering, Part A: Systems*, Vol. 147, No. 6, 2021, p. 05021001.
37. Ban, X. J., P. Hao, and Z. Sun, Real time queue length estimation for signalized intersections using travel times from mobile sensors. *Transportation Research Part C: Emerging Technologies*, Vol. 19, No. 6, 2011, pp. 1133–1156.
38. Levin, M. W., J. Hu, and M. Odell, Max-pressure signal control with cyclical phase structure. *Transportation Research Part C: Emerging Technologies*, Vol. 120, 2020, p. 102828.

39. Mousavizadeh, O., M. Keyvan-Ekbatani, and T. M. Logan, Real-time turning rate estimation in urban networks using floating car data. *Transportation research part C: emerging technologies*, Vol. 133, 2021, p. 103457.
40. Liu, H. and V. V. Gayah, Total-delay-based max pressure: a max pressure algorithm considering delay equity. *Transportation Research Record*, Vol. 2677, No. 6, 2023, pp. 324–339.
41. Lopez, P. A., M. Behrisch, L. Bieker-Walz, J. Erdmann, Y.-P. Flötteröd, R. Hilbrich, L. Lücken, J. Rummel, P. Wagner, and E. Wießner, Microscopic traffic simulation using sumo. In *2018 21st international conference on intelligent transportation systems (ITSC)*, IEEE, 2018, pp. 2575–2582.